Observations of Wind-Generated Waves on Variable Current

STEVEN R. LONG[1] AND NORDEN E. HUANG

NASA Wallops Flight Center, Wallops Island, Va. 23337

23 February 1976 and 31 May 1976

ABSTRACT

Laboratory measurements utilizing a laser probe are made for the slopes of wind waves generated on both positive and negative currents at different values of fetch. The data are then processed electronically to yield an average wave-slope spectrum in frequency space with 128 degrees of freedom. These spectra are used to obtain the growth of the spectral components at various frequency bands for increasing wind and different values of fetch and current. The results indicate that the growth of these components is not monotonic with the frictional wind speed U_*, but rather exhibits an "overshoot" phenomena at lower values of U_*, and in addition, displays a significant effect due to current. The peak location and spectral intensity of the spectra also show strong influence by the current condition. This results in the rms surface slope value increasing with negative current and decreasing with positive current. The results agree qualitatively with some theoretical predictions. The potential use of the current-induced effects as a means for remote sensing of ocean current is also briefly discussed.

1. Introduction

In recent years much attention has been directed toward both theoretically predicting and experimentally observing waves in the higher wavenumber range, where the surface tension force cannot be neglected. This has been due in part to the development and ongoing improvement of various microwave devices for remotely measuring the ocean surface characteristics. These devices are particularly responsive to this higher wavenumber range due to Bragg scattering. In previous studies and observations, most efforts and the results that have been produced were concerned primarily with gaining knowledge and insight into the problem of wind waves and wave behavior in general, in the absence of current (cf. Phillips, 1966). Because in the earth's oceans there are locations where waves are both generated and maintained on strong currents, there still exists a need for understanding how wave characteristics are changed or modified in the presence of current.

A recent study by Strong and DeRycke (1973) found that under proper conditions, changes of wave structure over the Gulf Stream gave a stronger signal of the current than did the surface infrared imagery. Also Schumann (1975) reported some unusual sea conditions off the Cape of Good Hope caused by adverse wind and current-wave interactions along the Agulhas current. All these indicate not only the importance of current-wave interactions as a central problem in basic wave dynamics, but also the possibility of using its effect as a means of detecting current conditions by remote sensing techniques as suggested by Huang *et al.* (1972), Strong and DeRycke (1973) and McGoogan (1975).

The present study reports the results of a preliminary laboratory study examining the effects of both positive and reverse, or negative, currents on the characteristics of wind-generated waves as compared with the case for no current. In particular, the surface slope spectrum and total rms slope values are observed as they changed under these different conditions of wind, current and fetch. The surface slope is here measured due to its being a more representative quantity in the range of high wavenumbers.

2. Experimental setup

The wind, wave and current interaction tank at North Carolina State University was used in this study. The tank itself has a cross section of 61 by 91 cm, and a length of 15.2 m, as shown in Fig. 1. Because of the presence of the paddle (not used here), air intake and beach, the actual usable length for the wind waves was 7.0 m. The tank is equipped with a centrifugal pump which recirculates the water through a system of 15.2 cm (6 inch) diameter pipe and valves, producing a reverse flow (against the waves) of 2687 ℓ min^{-1} and a flow with the waves of 2839 ℓ min^{-1}, as determined from a Rockwell model 101 Mainline meter (rotor-type). The flow was smoothed near the output and in the absence of wind was observed to disturb the otherwise smooth surface only

[1] NRC Research Associate at NASA Wallops Flight Center.

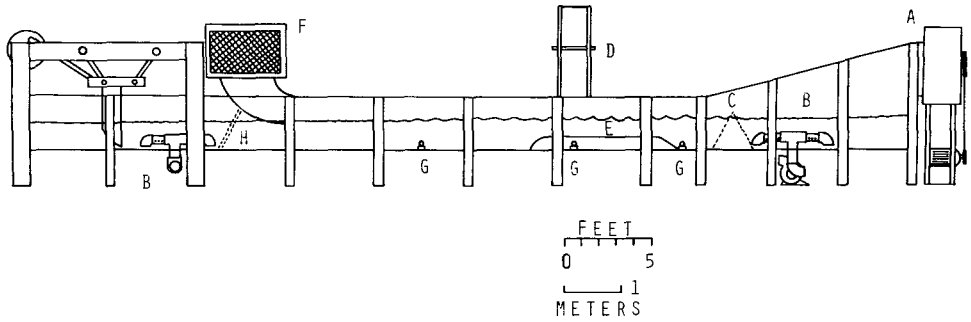

FIG. 1. The wind, wave and current interaction tank at North Carolina State University.

slightly. The resulting current values thus represent the mean flow. By using a plexiglass false bottom this resulted in a mean reverse flow of 28 ± 1 cm s^{-1} over the false bottom. Additionally, by means of the valves, the flow was reduced somewhat to an intermediate value, producing a reverse flow, or negative current of 22 ± 1 cm s^{-1} and a positive flow of 22 ± 1 cm s^{-1} over the false bottom. Throughout the remainder of the tank where the false bottom was not present, the current was correspondingly reduced. For each case of wind and fetch, the zero current case was observed in addition to the cases with current.

Three fetches at 2.59, 4.65 and 6.68 m were used. The fetch of 4.65 m was used in both the positive and reverse flow cases, and corresponded to a common point over the false bottom. The fetch of 2.59 m was used for positive flow, and was located just upstream and upwind of the false bottom. Likewise, the fetch of 6.68 m was used for reverse flow, and was located just upstream (but downwind) of the false bottom. Since the false bottom was not symmetrical along the current direction, but had a preferred direction of flow, it was oriented according to the flow direction used to ensure a smooth flow. For both orientations, the laser beam passed through the same point on the false bottom.

Prior to the measurements for each case studied, water was sampled near the beach area under steady wind conditions. These samples were then measured with a Cenco model 70530 du Noüy tensiometer. Thus surface tension was regularly checked to insure the best possible conditions. These values appear in Table 1.

To make the necessary measurements of wind waves under different current conditions, a laser beam of diameter ~0.5 mm was used as an optical probe. The beam was passed horizontally into the tank through the glass side, near the bottom, and deflected vertically upward by a first-surface mirror. Thus, at the air-water interface, refraction occurs as the various wave slopes pass the beam location. By using such an optical probe, many difficulties caused by the spot size of probes which physically penetrate the interface were avoided. Additionally, the problem which would be caused by the current flowing past a probe penetrating the interface did not arise. The detailed measuring techniques and procedures used here are the same as those reported in Long and Huang (1976).

3. Results and discussion

In the high-wavenumber range where capillary force is dominating, the asymptotic shape of the slope spectrum for the case of no current was proposed by Phillips (1966) to be of the form

$$S_{\alpha\beta}(N)=C_{\alpha\beta}N^{-1}, \tag{1}$$

for $N_m\ll N\ll N_\nu$, and where N_m is the frequency of the wave of minimum phase speed, N_ν represents a typical viscous wave frequency and $C_{\alpha\beta}$ represents universal constants, where α and β equal to 1 or 2, indicating the slope component direction.

To observe the case for no current, the photodiode array was positioned to receive the down-channel component of the slope signal (parallel with the mean wind). Fig. 2 gives the resulting down-channel frequency spectra of slope, $S_{11}(N)$, for a fetch of 4.65 m and no current. Wind speed was increased from 3.28 m s^{-1} ($U_*=15.2$ cm s^{-1}) to 12.29 m s^{-1} ($U_*=108$ cm s^{-1}). From this figure, several features are immediately evident. As discussed in detail by Long and Huang (1976), the envelope of the spectra compares favorably with an N^{-1} curve up to a frequency of about 30 Hz. Above this, an N^{-2} trend appears to be indicated. Because of this changing slope of the envelope, a more general form for the spectrum in this capillary-gravity range of higher wavenumbers was proposed by Long and Huang (1976) as

$$S_{11}(N)=f(U_*,\gamma,g)\frac{1}{N^{1+M}}, \tag{2}$$

where $f(U_*,\gamma,g)$ is a dimensional coefficient function for a power law spectrum, where U_* is frictional velocity, γ surface tension and g gravitational acceleration.

If we now include the effect of a positive current (in the direction of wind and waves) at the same location as in Fig. 2, the resulting spectral develop-

TABLE 1. Surface tension values from du Noüy tensiometer measurements.

Fetch (m)	U_* (cm s^{-1})	Surface tension τ (dyn cm^{-1} at 25.0°C)
4.65	15.8, 18.2, 21.4, 25.0, 29.4,	71.57
	32.8, 37.2, 53.0, 70.2,	72.00
	82.9, 102	72.00
6.68	15.0, 17.7, 20.8, 24.0	72.00
	27.3, 32.0, 36.5	71.89
	51.5, 67.5, 87.0, 108	72.00
4.65	15.2, 17.8, 20.1, 24.0, 28.5, 33.0, 36.4, 50.2, 64.5, 83.0, 108	72.00
2.59	15.5, 18.8, 21.0, 24.7, 28.5, 33.5, 39.0, 54.0, 68.0, 86.0, 107	71.79

ment with wind appears as Fig. 3. Here waves are generated and maintained on a mean current of 16 ± 0.5 cm s^{-1} and encounter 29 ± 1 cm s^{-1} of positive current over the false bottom, where the measurements were made. The identical range of wind speeds was used and the same values throughout the range, but as can be seen in Fig. 3, spectral development occurs differently and slower. Even with a slower development, an approach to an eventual equilibrium appears to be indicated. The form of the spectrum at each wind value appears changed when compared to Fig. 2. The peak of maximum slope values is broadened

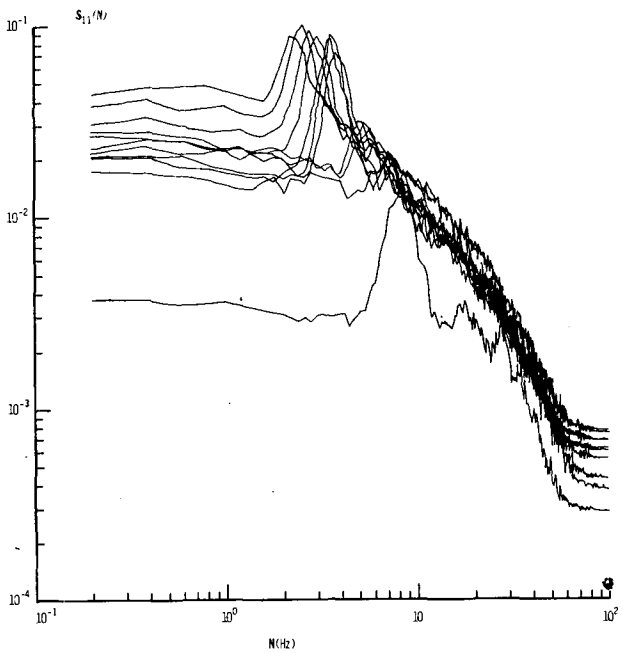

FIG. 2. The down-channel frequency spectrum of slope $S_{11}(N)$ under the influence of increasing wind. Fetch is constant at 4.65 m with no current. Increasing wind values are $U_*=15.2$, 17.8, 20.1, 24.0, 28.5, 33.0, 36.4, 50.2, 64.5, 83.0 and 108 cm s^{-1}.

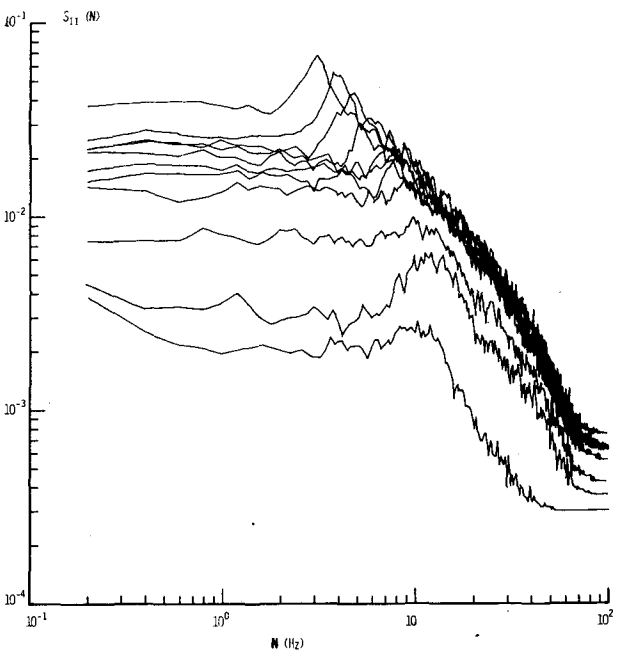

FIG. 3. As in Fig. 2 except under the influence of constant positive current. Current is 29 ± 1 cm s^{-1}.

about N_0. As wind increases, there is an initial shift toward higher frequency which finally reverses itself as the higher U_* values are approached.

Considering now the case of reverse or negative current, the wind speed set used in Figs. 2 and 3 was duplicated as closely as possible, ranging from 3.37 m s^{-1} ($U_*=15.8$ cm s^{-1}) to 12.9 m s^{-1} ($U_*=102$ cm s^{-1}) in nearly identical steps. Waves were generated on a mean reverse current of 15 ± 0.5 cm s^{-1} and encountered 28 ± 1 cm s^{-1} over the false bottom, where the slopes refracted the laser beam. The resulting spectral growth with wind is given by Fig. 4. Even the lower wind speed values produce a spectrum similar in form to the higher wind speed spectra for no current. Particular to the reverse case as seen in Fig. 4, the peaks of maximum slope all group together around a similar frequency. Even in allowing for a surface drift current induced by the wind which would increase for increasing wind, one cannot conclude that this would account for what is observed in Fig. 4. A possible explanation for this is found in Guttman (1972) who plotted wavenumber K against frequency N with current speed as a parameter. The resulting figure displays a region where change is slow in frequency for a much larger change in K for a negative current similar in value to that used here. This would allow for a change in wavenumber K, and thus the wavelength, without a correspondingly rapid change in frequency.

If a line were now to be fitted over these slope spectra from the peak to the high frequency region, then this line could represent an asymptotic equi-

librium envelope, the final level suggested by these observations. As can be seen in the previous figures, the slope of this line would change. Such a fit was done to the spectra of these observations. The slope of this line was called $(1+M)$, as suggested by Eq. (2). Also, the intersection of this line with the vertical axis at $N=1$ Hz was called $S_{11}{}^*(1)$. Since current has been seen to affect the slope spectra in various ways, a modification to Eq. (2) is suggested in the form of

$$S_{11}(N)=F(U_*,V,\gamma,g)\frac{1}{N^{1+M}}. \tag{3}$$

As before, γ and g are included due to their importance in wind waves, as discussed by Phillips (1958, 1966). Recently, Banner and Phillips (1974) and Phillips and Banner (1974) have made further suggestions about the importance of the surface drift current and preexisting swell on the capillary-gravity wave stability. Surface drift and U_* are directly related, thus the inclusion of U_* in Eq. (3). Preexisting swell may be specified by N_0. In the present study, however, there was no preexisting swell. All waves present were wind-generated with U_* determining the value of N_0. Then for the case $N=1$ Hz, (3) becomes

$$S_{11}(1)=F(U_*,V,\gamma,g)\equiv S_{11}{}^*(1), \tag{4}$$

so that $S_{11}{}^*(1)$ is the coefficient associated with the equilibrium range.

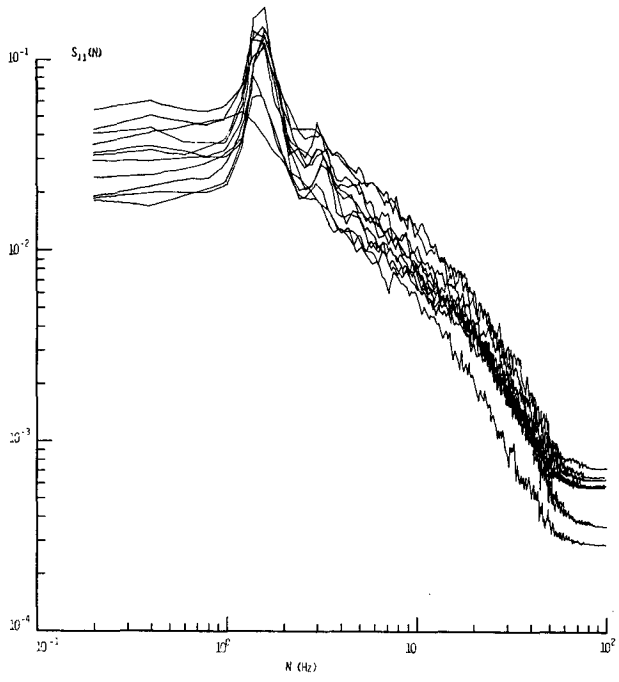

FIG. 4. As in Fig. 2 except under the influence of constant negative current. Increasing wind values are $U_*=15.8$, 18.2, 21.4, 25.0, 29.4, 32.8, 37.2, 53.0, 70.2, 82.9 and 102 cm s^{-1}. Current is 28 ± 1 cm s^{-1}.

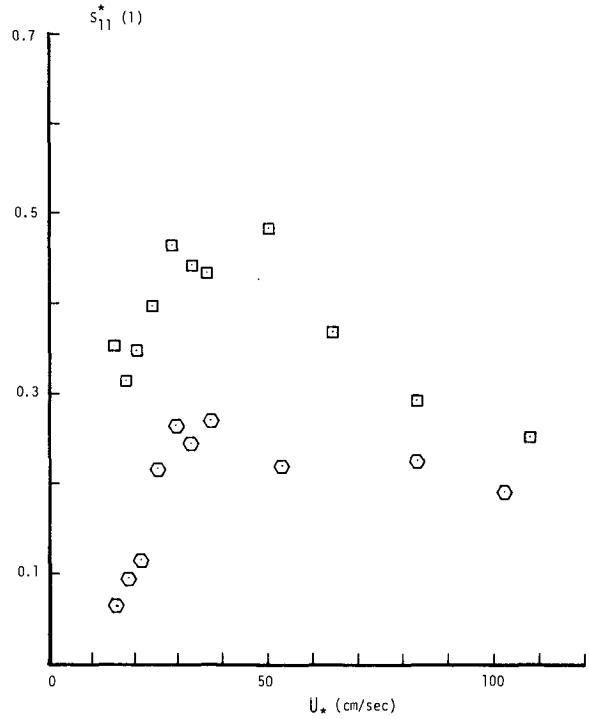

FIG. 5. The variation of $S_{11}{}^*(1)$ with U_* and current. Fetch is constant at 4.65 m. Currents are positive current of 29 ± 1 cm s^{-1} (⊡) and negative current of 28 ± 1 cm s^{-1} (⊙).

Using this method of fitting a straight line envelope over the spectra, $S_{11}{}^*(1)$ was obtained, and appears as Fig. 5. In both the positive and negative current cases, a rapid growth with the initial increase of U_* is observed, resulting in an overshoot and decline. For higher U_* values, the results for positive and negative current approach each other as the value 0.2 for $S_{11}{}^*(1)$ is approached. At all values other than those approaching high wind speeds, current appears to cause a difference in the $S_{11}{}^*(1)$ values observed.

From the same line that determined $S_{11}{}^*(1)$, the quantity M was obtained from its slope, $(1+M)$. M appears as Fig. 6. Below $U_*=30$ cm s^{-1}, positive and negative current exhibit an opposite influence.

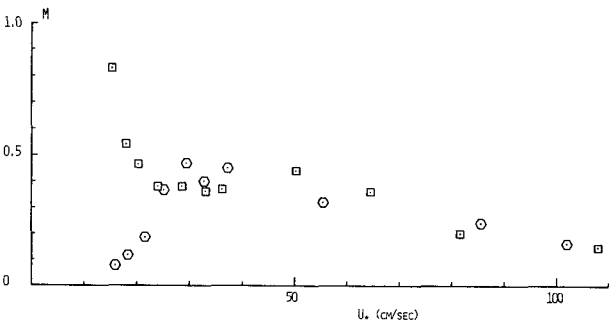

FIG. 6. The variation of M and U_* and current. Fetch is constant at 4.65 m. Currents are positive current of 29 ± 1 cm s^{-1} (⊡) and negative current of 28 ± 1 cm s^{-1} (⊙).

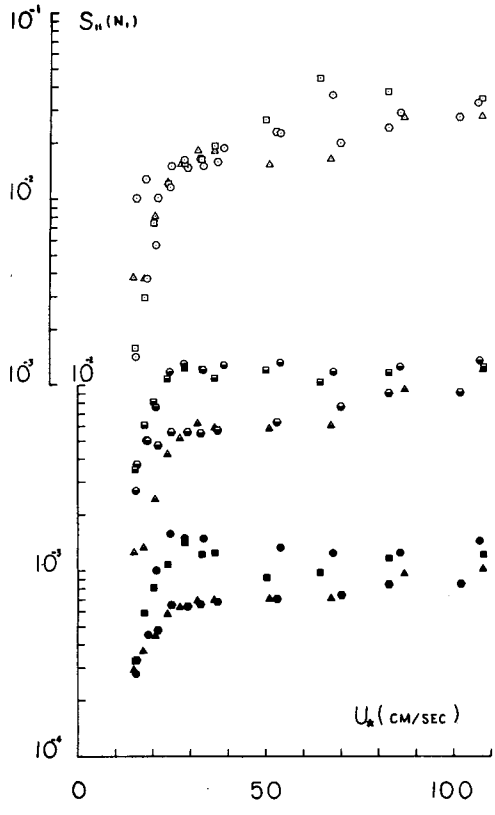

FIG. 7. The growth of spectral components within a frequency band $S_{11}(N_1)$ with increasing U_* for $N_1=5$ Hz. Fetch and current values are 2.59 m and $+16\pm0.5$ cm s^{-1} (⊙), 4.65 m and $=29\pm1$ cm s^{-1} (⊡), 4.65 m and -28 ± 1 cm s^{-1} (⊙), and 6.68 m and -15 ± 0.5 cm s^{-1} (△). For $N_1=13.5$ Hz, fetch and current values are 2.59 m and $+16\pm0.5$ cm s^{-1} (◒), 4.65 m and $+29\pm1$ cm s^{-1} (◘), 4.65 m and -28 ± 1 cm s^{-1} (◒), and 6.68 m and -15 ± 0.5 cm s^{-1} (▲). For $N_1=56$ Hz, fetch and current values are 2.59 m and $+16\pm0.5$ cm s^{-1} (●), 4.65 m and $+29\pm1$ cm s^{-1} (■), 4.65 m and -28 ± 1 cm s^{-1} (●), and 6.68 m and -15 ± 0.5 cm s^{-1} (▲).

However, above about 30 cm s^{-1} for U_*, the resulting M values are practically the same for both positive and negative current. As U_* increases, M is seen to approach zero, indicating that

$$\frac{1}{N^{1+M}} \text{ approaches } \frac{1}{N} \text{ for increasing } U_*.$$

Considering now the growth of spectral components within a frequency band, Fig. 7 shows the growth observed in the components of frequency 5, 13.5 and 56 Hz. These frequencies correspond to contributions by surface tension or capillary forces of 10%, 50% and 90%, respectively. For the 5 Hz components after a rapid growth in the initial U_* range, a slower rate of steady increase develops. It is only in the intermediate range of U_* that any difference due to positive or negative current is observed. Rapid early growth is also observed in the 13.5 Hz range. Positive and negative current can be seen to have different effects on growth until the higher U_* levels are reached. There, current effects aren't as noticeable. Even at higher frequency (56 Hz) the effect of different current directions can be seen throughout the range of U_* observed, after initial growth. Thus in the development of spectral components, an important role for current is implied by the observations.

To illustrate the effect of different currents and fetch on the peak frequency N_0, Fig. 8 shows its change with current, increasing U_* and fetch. Fetches of 2.56, 4.65 and 6.68 m are used with positive and negative currents. The location of N_0 for the negative currents changes very little for increasing U_*. The trends observed here imply a common level of N_0 or at least a similar value at higher U_*, regardless of the current condition. Although this study did not go higher than $U_*=108$ cm s^{-1}, the present data seems to indicate this trend.

The contribution of the Doppler shift to the frequency changes is also indicated in Fig. 8. While the results give good agreement in the positive current cases, the agreement in the negative current cases is rather poor. This may be explained by Phillips' (1974) study, which indicated that for the case of either very fast internal waves or the presence of negative surface currents, the wavelengths involved in direct resonance are no longer short enough to be masked by the energy input from the wind. Additional studies are planned to clarify this in the future.

To reexamine the fetch information, the nondimensional fetch gX/U_*^2 was formed and compared with

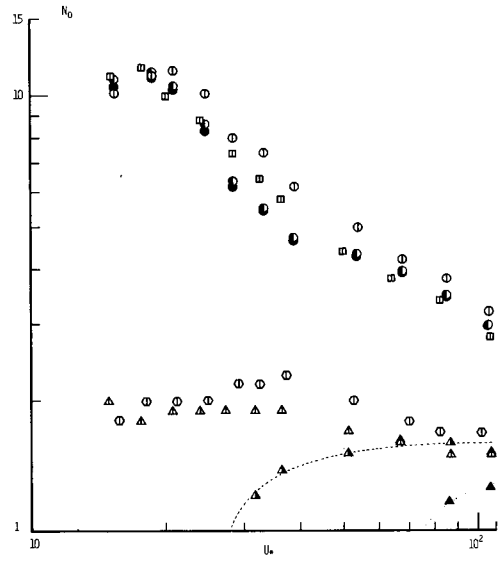

FIG. 8. The change of the peak frequency N_0 with current, fetch and increasing U_*. Fetch and current values are at 2.59 m, $+12\pm0.5$ cm s^{-1} (◑); at 4.65 m, $+22\pm1$ cm s^{-1} (◫), -22 ± 1 cm s^{-1} (◭); and at 6.68 m, -12 ± 0.5 cm s^{-1} (◬). The values predicted by a Doppler shifts are at 2.59 m, $+16\pm0.5$ cm s^{-1} (●), $+12\pm0.5$ cm s^{-1} (◐); and at 6.68 m, -15 ± 0.5 cm s^{-1} (▲), -12 ± 0.5 cm s^{-1} (◭).

the nondimensional frequency N_0U_*/g (see Fig. 9). The data for zero current follows well the proposed empirical formulas of previous studies, such as Mitsuyasu (1968) and Kitaigorodskii (1970), exhibiting a slope of $-\frac{1}{3}$ up to the critical value, where it suddenly changes, as discussed by Long and Huang (1976). The current data, however, cannot be said to follow the empirical formulas as previously proposed. The cases of positive current appear to follow a slope of approximately $-\frac{1}{7}$, while the negative or reverse current data lie along a slope of about $-\frac{1}{2}$. This reflects the clearly different trends as illustrated in Figs. 2, 3 and 4. Thus from Fig. 9 the effect of current is again clearly noticeable.

Considering now the total rms slope $\overline{(\nabla\zeta)^2}$ obtained as the vector sum of the down-channel component $S_{11}(N)$ values and the across-channel component $S_{22}(N)$ values, its change with U_* is illustrated by Fig. 10. The negative or reverse current data are seen to be consistently higher than the positive current data at each U_* value throughout the range of U_*. The fetch was constant at 4.65 m.

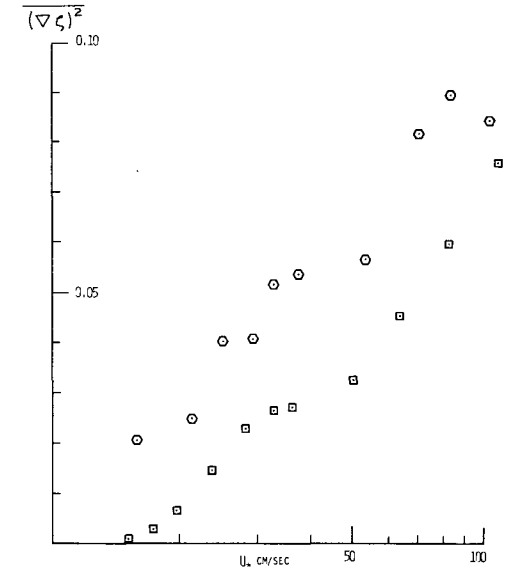

FIG. 10. The total rms slope $\overline{(\nabla\zeta)^2}$ as it changes with U_*. Fetch is constant at 4.65 m. Currents are $+29\pm1$ cm s^{-1} (⊡) and -28 ± 1 cm s^{-1} (◇).

4. Summary

The results of the present study indicate that the effect of current on wind-generated waves is not negligible. For positive currents, the development of the slope spectra with increasing wind was noticeably different from the case with no current. An even greater difference was noted for negative current. The peak frequency N_0, or the frequency of the maximum slope, was observed to vary only slightly from the smallest to the largest U_* used. In comparing the data in nondimensional form, a significant difference due to current was noted when compared with earlier results for no current.

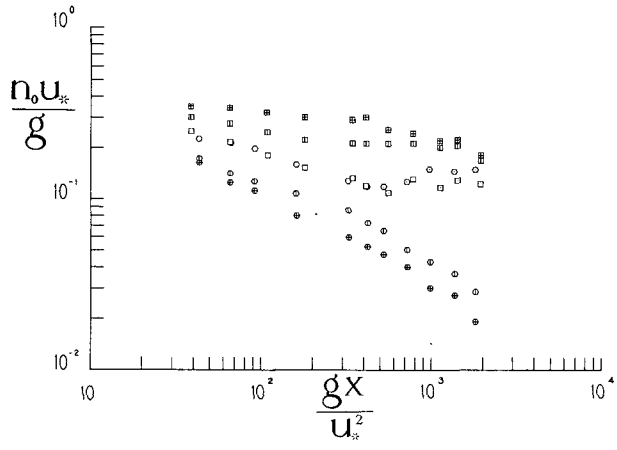

FIG. 9. The nondimensional fetch gx/U_*^2 as it changes with nondimensional frequency N_0U_*/g. Here $u_*=U_*$, $n_0=N_0$. Data taken at fetch $=4.65$ m for the current values: $+29\pm1$ cm s^{-1} (⊞), $+22\pm1$ cm s^{-1} (⊡), no current (⊡,◇), -28 ± 1 cm s^{-1} (⊕), and -22 ± 1 cm s^{-1} (◫).

The growth of the spectral components was examined for different frequency bands and found to be not monotonic, but rather to display an "overshoot" following a rapid growth in the low U_* range. This "overshoot" was followed by a more gradual growth up to the limit of U_* used in the study. The effects of current were again noticeable here until the maximum U_* was approached. Negative current reduced the growth and positive current augmented it as U_* increased.

The rms surface slope was also observed to change with current. An increase was noted when negative currents were present, and a corresponding decrease for positive currents.

These preliminary observations indicate that current definitely affects the characteristics of wind-generated waves in a systematic way that is readily observable. If currents are present either in the laboratory or in field studies, these results imply that they must be taken into account to properly interpret the data.

This brings us back to the problem of remote sensing techniques briefly described at the beginning. Granted that most theoretical analyses on current-wave interaction problems emphasize the importance of the current gradient (Longuet-Higgins and Stewart, 1961; Kenyon, 1971; Huang *et al.*, 1972), yet the length scale required to produce the velocity gradient that can be felt by the high-frequency capillary-gravity waves is too small to exist at the current boundary in the natural environment. However, changes in the capillary-gravity wave structure and hence the surface

roughness do occur. The possible explanations for this are probably due to the following:

1) Indirect cause. Although the life spans of the capillary-gravity waves are short, the pure gravity waves are long enough to be influenced by the current gradient. The capillary-gravity waves would then be changed by wave-wave interactions in this indirect way.

2) Direct cause. When water is moving at a speed of the order of 2 m s^{-1}, as in the Gulf Stream, turbulence will inevitably be generated. Usually the oceanic turbulence scales are too small and their intensity too weak to influence the gravity waves. But for the capillary-gravity waves the relative ratio may change. Then direct turbulence-wave interactions similar to that discussed by Phillips (1959) will become the dominant mechanism. Unfortunately, there are no data yet to test these hypotheses.

It is the cumulative effect of the current gradient through the transitional section of the false bottom that is clearly observed here. Such an effect should be equally observable in the ocean. In fact, the studies by Strong and DeRycke (1973) and McGoogan (1975) both indicated that changes in the wave structure at strongly concentrated current systems were clearly observable not only at the edge but also in the current system proper. Their measurements were by sunglint with a very high resolution radiometer on the NOAA-2 satellite and by the radar reflectivity with the automatic gain control (AGC) circuit of the altimeter on Skylab. Although all these results are still qualitative, the effect, if clearly understood and accurately calibrated, can be used as a possible means of current detection in the ocean by various remote sensing techniques.

The present paper reports an initial effort in this direction to call attention to these problems. Due to the limitations on resources and time in the study, the important aspect of the detailed dynamics involving the current gradient has not been fully explored. Additional study on the dynamics is planned in a new wind-wave-current interaction channel now under construction.

Acknowledgments. The authors wish to express their appreciation for the assistance and help provided by Dr. F. Y. Sorrell and Mr. Andrew Withers during the experimental phase of the study, and Messrs. C. Parsons and J. T. McGoogan for valuable suggestions for the manuscript. Gratitude is also expressed by SRL for the support provided by Contract NAS6-2617 from the NASA Wallops Flight Center, for the support provided by the Center for Marine and Coastal Studies, North Carolina State University, and for the helpful cooperation of the Department of Geosciences, North Carolina State University.

REFERENCES

Banner, M. L., and O. M. Phillips, 1974: On the incipient breaking of small scale waves. *J. Fluid Mech.*, **65**, 647–656.

Guttman, N. B., 1972: On the non-linear dispersive relationship in a random surface gravity and capillary wave field. Ph.D. thesis, North Carolina State University.

Huang, N. E., D. T. Chen, C. C. Tung and J. R. Smith, 1972: Interactions between steady non-uniform currents and gravity waves with applications for current measurement. *J. Phys. Oceanogr.*, **2**, 420–431.

——, F. Y. Sorrell, C. C. Tung, N. Gutman, S. R. Long and G. V. Sturm, 1974: Ocean dynamics studies of current-wave interactions. NASA CR-137467, 180 pp.

Kenyon, K. E., 1971: Wave refraction in ocean currents. *Deep-Sea Res.*, **18**, 1023–1034.

Kitaigorodskii, S. A., 1970: *The Physics of Air-Sea Interaction.* Leningrad. [Jerusalem, Keter Press], 237 pp.

Long, S. R., and N. E. Huang, 1976: On the variation and growth of wave slope spectra in the capillary-gravity range with increasing wind. (Accepted for publication in *J. Fluid Mech.*)

Longuet-Higgins, M. S., and R. W. Stewart, 1961: The changes in amplitude of short gravity waves on steady non-uniform currents. *J. Fluid Mech.*, **10**, 529–549.

McGoogan, J. T., 1975: Satellite altimetry applications. *IEEE Trans. Microwave Theory Tech.*, **MTT-23**, 970–978.

Mitsuyasu, H., 1968: On the growth of the spectrum of wind generated waves. *I. Reps. Res. Inst. Appl. Mech. Kyushu Univ.*, **16**, 459–482.

Phillips, O. M., 1958: The equilibrium range in the spectrum of wind-generated waves. *J. Fluid Mech.*, **4**, 426–434.

——, 1959: The scattering of gravity waves by turbulence. *J. Fluid Mech.*, **5**, 177–192.

——, 1966: *The Dynamics of the Upper Ocean.* Cambridge University Press, 261 pp.

——, 1974: Surface effects: An analysis and review of the processes involved and phenomena observed. Hydronautics, Inc. Tech. Rep. 7211-9, NTIS AD/A-004 956, 93 pp.

——, and M. L. Banner (1974). Wave breaking in the presence of wind drift and swell. *J. Fluid Mech.*, **66**, 625–640.

Schumann, E. H., 1975: High waves in the Agulhas current. *The South African Shipping News and Fishing Industry Rev.* March, 25–27.

Strong, A. E., and R. J. DeRycke, 1973: Ocean current monitoring employing a new satellite sensing technique. *Science*, **182**, 482–484.

Wu, J., 1968: Laboratory studies of wind-wave interactions. *J. Fluid Mech.*, **34**, 91–111.